AMERICAN SOCIETY FOR MICROBIOLOGY | Molecular and Cellular Biology®

RESEARCH ARTICLE

Triptolide-Assisted Phosphorylation of p53 Suppresses Inflammation-Induced NF-κB Survival Pathways in Cancer Cells

Li Zheng,[a] Jia Jia,[b] Huifang Dai,[a]* Lei Wan,[a,c] Jian Liu,[c] Lin Hu,[d] Mian Zhou,[a] Michael Qiu,[a] Xufeng Chen,[a]* Lufen Chang,[a] Jae Y. Kim,[e] Karen Reckamp,[f] Dan J. Raz,[e] Zongping Xia,[d] Binghui Shen[a]

Departments of Cancer Genetics and Epigenetics,[a] Surgery,[e] and Medical Oncology and Therapeutics Research,[f] City of Hope National Medical Center and Beckman Research Institute, Duarte, California, USA; Shanghai Center for Bioinformatics Technology, Shanghai, China[b]; First Affiliated Hospital, Anhui University of Chinese Medicine, Hefei, Anhui, China[c]; Life Science Institute, Zhejiang University, Hangzhou, Zhejiang, China[d]

ABSTRACT Chronic inflammation plays important roles in cancer initiation and progression. Resolving chronic inflammation or blocking inflammatory signal transduction may prevent cancer development. Here, we report that the combined low-dose use of two anti-inflammatory drugs, aspirin and triptolide, reduces spontaneous lung cancer incidence from 70% to 10% in a mouse model. Subsequent studies reveal that such treatment has little effect on resolving chronic inflammatory conditions in the lung, but it significantly blocks the NF-κB-mediated expression of proliferation and survival genes in cancer cells. Furthermore, triptolide and aspirin induce distinct mechanisms to potentiate each other to block NF-κB nuclear localization stimulated by inflammatory cytokines. While aspirin directly inhibits IκB kinases (IKKs) to phosphorylate IκBα for NF-κB activation, triptolide does not directly target IKKs or other factors that mediate IKK activation. Instead, it requires p53 to inhibit IκBα phosphorylation and degradation. Triptolide binds to and activates p38α and extracellular signal-regulated kinase 1/2 (ERK1/2), which phosphorylate and stabilize p53. Subsequently, p53 competes with IκBα for substrate binding to IKKβ and thereby blocks IκBα phosphorylation and NF-κB nuclear translocation. Inhibition of p38α and ERK1/2 or p53 mutations could abolish the inhibitory effects of triptolide on NF-κB. Our study defines a new p53-dependent mechanism for blocking NF-κB survival pathways in cancer cells.

KEYWORDS cancer, IκBα, NF-κB, triptolide, aspirin, inflammation, p53

Received 5 April 2017 **Returned for modification** 24 April 2017 **Accepted** 16 May 2017

Accepted manuscript posted online 22 May 2017

Citation Zheng L, Jia J, Dai H, Wan L, Liu J, Hu L, Zhou M, Qiu M, Chen X, Chang L, Kim JY, Reckamp K, Raz DJ, Xia Z, Shen B. 2017. Triptolide-assisted phosphorylation of p53 suppresses inflammation-induced NF-κB survival pathways in cancer cells. Mol Cell Biol 37:e00149-17. https://doi.org/10.1128/MCB.00149-17.

Address correspondence to Binghui Shen, bshen@coh.org.

* Present address: Huifang Dai and Xufeng Chen, Department of Pathology, Duke University, Durham, North Carolina, USA.

Cancer arises due to abnormally acquired genome instability, unlimited proliferation potential, resistance to growth inhibition and cell death, and an aberrant stromal microenvironment, all of which are characterized as cancer hallmarks (1). A remarkable feature of chronic inflammation is that it is able to trigger the expression of most of these cancer hallmarks (1). Inflammation from persistent bacterial or viral infection, environmental exposure, or genetic defects results in the proliferation and recruitment of immune cells, such as macrophages, to inflamed tissue sites (2, 3). These cells overexpress and secrete proinflammatory cytokines, such as tumor necrosis factor alpha (TNF-α), interleukin-1β (IL-1β), and IL-6, which promote cell proliferation and cell survival (2, 3). TNF-α, IL-1α, and IL-1β, upon binding to their cognate receptors, initiate signaling cascades that lead to the activation of transcription factors such as NF-κB (4). For instance, the binding of TNF-α to its receptor, TNF1R, triggers a conformational change in the receptor, recruiting proteins, including TRAF2/5 and RIP1. The subsequent ubiquitination of RIP1 by the cellular inhibitor-of-apoptosis proteins c-IAP1 and c-IAP2 and other E3 ubiquitin ligases leads to the recruitment of the IκB kinase (IKK)

complex (5). The IKK complex consists of two kinase components, IKKα and IKKβ, and one regulatory component, IKKγ (NEMO) (6). In addition, IL-1α and IL-1β bind to the IL-1 receptor (IL-1R) and recruit the adaptor proteins MyD88, IRAK4, and IRAK1, leading to the activation of the E3 ubiquitin ligase TRAF6. Activated TRAF6, together with the ubiquitin-conjugating enzyme E2 Ubc13/Uev1A heterodimer, catalyzes the synthesis of unanchored K63-linked polyubiquitin chains (5). These free polyubiquitin chains then function as secondary messenger-like molecules and bind to TAB2, the structural subunit of the TAK1 kinase complex, leading to the dimerization or oligomerization of the TAK1 complex and its autophosphorylation and activation (5). Activated TAK1 phosphorylates the IKK kinase complex. In both the TNF-α and IL-1 signaling pathways, activated IKKs then phosphorylate IκBα, leading to its ubiquitination and subsequent degradation by the proteasome (5). After IκBα degradation, NF-κB becomes free to translocate into the nucleus to mediate the expression of target genes. NF-κB activation has been shown to be a key molecular event during the development of chronic inflammation-associated cancer (7–9).

The causal roles of chronic inflammation in cancer initiation and progression provided the foundation for targeting inflammation-associated signaling pathways in cancer prevention and treatment (3, 10). Many anti-inflammatory chemicals are derived from natural sources and may be useful, either alone or in combination with other agents, as anticancer therapeutics. One such chemical is triptolide, a diterpenoid epoxide derivative of the anti-inflammatory herb *Tripterygium wilfordii* (thunder god vine). Triptolide has been used to treat rheumatoid arthritis and other inflammatory diseases in China for many years (11). Recent studies have shown that triptolide can kill multiple types of cancer cells *in vitro* with high potency (12–14). Furthermore, an animal study showed that triptolide can inhibit tumor formation and the growth of pancreatic cancer cells in a mouse xenograft model (15). Therefore, we tested triptolide alone and in combination with other putative anti-inflammatory agents to identify novel chemotherapeutic strategies.

In this study, we used an inflammation-associated spontaneous-cancer mouse model developed in our laboratory (9) to test candidate anti-inflammatory therapies for a role in preventing cancer. We discovered that triptolide, when combined with acetylsalicylic acid (aspirin) in low-dose dual therapy, dramatically blocked cancer cell proliferation *in vitro* and tumor formation *in vivo*. This effect was greater than expected based on the modest effects of either triptolide or aspirin alone. Combined therapy robustly blocked the expression of NF-κB-mediated proliferation and survival genes without resolving immune cell infiltration or cytokine production. Further mechanistic studies allowed us to shed light on how these two compounds potentiate the suppression of inflammation-induced NF-κB pathways in cancer cells. Consistent with previous findings, aspirin can inhibit IκBα phosphorylation and degradation. Surprisingly, we also found that triptolide blocked TNF-α- and IL-1β-induced NF-κB nuclear translocation in a p53-dependent manner. Via high-throughput computer- and phosphoprotein array-based screening assays, we discovered that triptolide activates extracellular signal-regulated kinase 1/2 (ERK1/2) and p38 mitogen-activated protein kinase (MAPK) signaling, which subsequently phosphorylates p53, leading to p53 stabilization and nuclear accumulation at a low dosage, which is nontoxic to normal cells. Our work demonstrates novel mechanisms for triptolide that, when combined with aspirin, lead to potent NF-κB inhibition and cancer suppression.

RESULTS

Low doses of triptolide and aspirin potentiate each other to suppress cancer development. We previously developed a chronic inflammation-associated lung cancer mouse model via the knock-in of a Fen1 (flap endonuclease 1) mutation (E160D), thereby modeling the Fen1 mutations that have been identified in human lung cancer and other cancer patients (9). We predicted that compounds that suppress inflammation or block inflammation-induced NF-κB survival pathways may be able to prevent and/or stop spontaneous lung cancer development. To test this hypothesis, we fed the

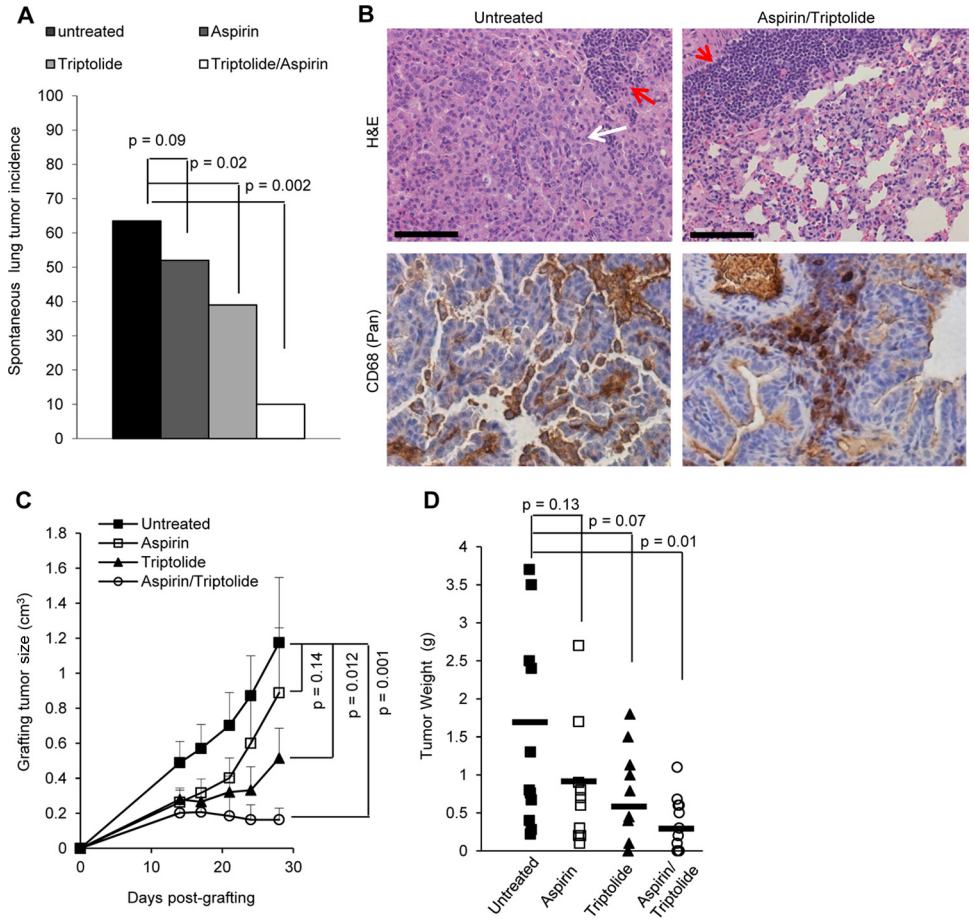

FIG 1 Low-dose triptolide and aspirin suppress lung cancer development. (A) Spontaneous tumor incidence in E160D FEN1 mutant mice that were gavage fed with triptolide (1 mg/kg body weight) and/or aspirin (4 mg/kg body weight) ($n = 30$ for each group). The tumor incidence in each group was determined by anatomic and histopathologic analyses. *P* values were calculated by two-sided Fisher's exact test. (B) Representative images of H&E staining and IHC staining of macrophages in lung tissue sections from mice without or with aspirin (4 mg/kg body weight) and triptolide (1 mg/kg body weight) feeding for 2 months. Bars, 50 μm. The white arrows and red arrows in the H&E-stained images indicate lung adenocarcinoma and T cell infiltrates, respectively, in lungs treated or not treated with aspirin-triptolide. Monocytes/macrophages were detected by using anti-CD68 antibody. (C and D) Tumor burdens in Lewis lung carcinoma-grafted mice not treated or treated with triptolide and/or aspirin ($n = 10$ for each group). (C) Mean tumor sizes ± standard errors of the means for each group of mice during treatments. (D) Tumor weight of each mouse at the terminal stage. *P* values were calculated by Student's *t* test.

E160D mutant with triptolide or the traditional anti-inflammatory compound aspirin individually or in combination. A total of 63.3% of untreated control E160D mice (19 out of 30) developed lung adenomas and adenocarcinomas (Fig. 1A). Aspirin and triptolide reduced the lung cancer frequency by 14% ($P = 0.09$) and 42% ($P = 0.02$), respectively. Interestingly, the combined administration of aspirin and triptolide reduced the number of tumor-bearing mice by 84%, reducing the tumor incidence to 10% ($P = 0.002$) (Fig. 1A). This effect was substantially greater than the predicted additive effect based on administration. Analysis of variance (ANOVA) (two factors with replication) indicated a significant interaction between aspirin and triptolide, with a *P* value of <0.0001. However, combined treatment with low-dose aspirin-triptolide did not reduce the levels of T cell infiltrates or $CD68^+$ monocytes/macrophages (Fig. 1B), suggesting that low-dose aspirin-triptolide did not resolve chronic inflammation in the lung. Instead, they might directly suppress tumor cell survival and growth. Supporting this hypothesis, we observed that the combined use of triptolide and aspirin significantly inhibited tumor growth of grafted Lewis lung carcinoma cells in mice (Fig. 1C and D).

To further investigate how triptolide and aspirin together suppress lung cancer development in mice, we compared the gene expression profiles for E160D mice (10

months old) that were either untreated or treated with aspirin, triptolide, or aspirin-triptolide for 2 months, when chronic inflammation was present but no adenomas were detectable. We conducted Ingenuity Pathway Analysis on significantly upregulated genes (fold change [treatment versus control] of >1.5 and *P* value of <0.05) or downregulated genes (fold change [treatment versus control] of <0.67 and *P* value of <0.05) to identify the pathways that were affected by aspirin, triptolide, or the combination of aspirin and triptolide. A low dose of aspirin alone significantly downregulated genes related to inflammatory responses (3 genes) and the cell survival pathway (9 genes). Upstream regulator analysis revealed that vascular endothelial growth factor (VEGF) signaling was predicted to be inhibited by aspirin alone ($P < 0.05$). Similarly, a low dose of triptolide alone significantly downregulated the genes responsible for inflammation responses (4 genes), cell survival (5 genes), and cancer (6 genes). TNF-α signaling was predicted to be inhibited by triptolide ($P < 0.05$). Intriguingly, the administration of low-dose aspirin-triptolide downregulated 265 cancer-related genes. Of these cancer-related genes, 74 and 155 genes were associated with cell survival and cell growth and proliferation, respectively. Upstream regulator analysis pointed to an inhibition of the cell proliferation and survival pathways that are mediated by TNF-α, IL-1β, transforming growth factor β (TGF-β), and VEGF in the lungs of mice treated with triptolide and aspirin ($P < 0.05$) (Fig. 2A). The transcription factors NF-κB, SP1, and HIF1 were major downstream nodes in these downregulated signaling pathways, controlling the expression of genes that regulate cell proliferation and survival (Fig. 2A). Consistent with the microarray data, immunohistochemical staining for NF-κB revealed a nuclear staining pattern in the lung tissues of control E160D mice but a cytoplasmic NF-κB staining pattern in the lung tissues of aspirin-triptolide-treated mice, indicating that NF-κB was inactive (Fig. 2B). In addition, we found that aspirin-triptolide effectively blocked the TNF-α-induced nuclear translocation of NF-κB (Fig. 2C). These data suggest that low-dose aspirin-triptolide does not effectively reduce the levels of proinflammatory cells, such as T cells and macrophages, nor does it decrease the overall levels of proinflammatory cytokines in the lung. However, combined treatment might inhibit key downstream transcription factors such as NF-κB to block the induction of cell proliferation and survival pathways by these proinflammatory cytokines in precancerous and cancer cells (Fig. 2D).

Triptolide and aspirin block cytokine-induced NF-κB nuclear translocation and activation. We then investigated the impact of low-dose aspirin-triptolide on NF-κB activation by proinflammatory cytokines in human lung cancer cells. In H460 cells not stimulated by TNF-α or IL-1β, NF-κB was located in the cytoplasm (Fig. 3A), and triptolide or aspirin had little effect on the status of NF-κB (data not shown). In H460 cells stimulated by TNF-α or IL-1β, NF-κB translocated into the nuclei, but pretreatment of cancer cells with triptolide for 16 h inhibited IκB degradation (Fig. 3A) and impaired NF-κB nuclear translocation in response to TNF-α or IL-1β (Fig. 3A to C). Interestingly, unlike triptolide, aspirin effectively blocked IL-1β-induced but only mildly inhibited TNF-α-induced IκBα degradation and NF-κB nuclear translocation in H460 lung cancer cells (Fig. 3A to C). However, when the cells were treated with both triptolide and aspirin, there was a potentiation effect on NF-κB nuclear translocation (Fig. 3A to C), because ANOVA (two factors with replication) indicated a significant interaction between aspirin and triptolide, with *P* values of 0.0001 and 0.027 for the IL-1β and TNF-α induction assays, respectively. A similar observation was made with sodium salicylate, an aspirin derivative that does not inhibit Cox-2.

Triptolide blocks TNF-α-induced NF-κB nuclear translocation in a p53-dependent manner. Next, we addressed the critical issues of how triptolide and aspirin can individually inhibit NF-κB nuclear translocation and how they potentiate each other when combined. To investigate the impact of aspirin and triptolide on IKK activation, we used the cell-free TRAF6-depedent IKK activation assay system (16) to monitor the phosphorylation of IκBα. As a positive control, the addition of TRAF6 to the cytoplasmic fraction (S100) of cell extracts activated IKKβ, leading to IκBα phosphorylation (Fig. 3D, lane 2). Meanwhile, either aspirin or sodium salicylate, the main metabolite of aspirin in

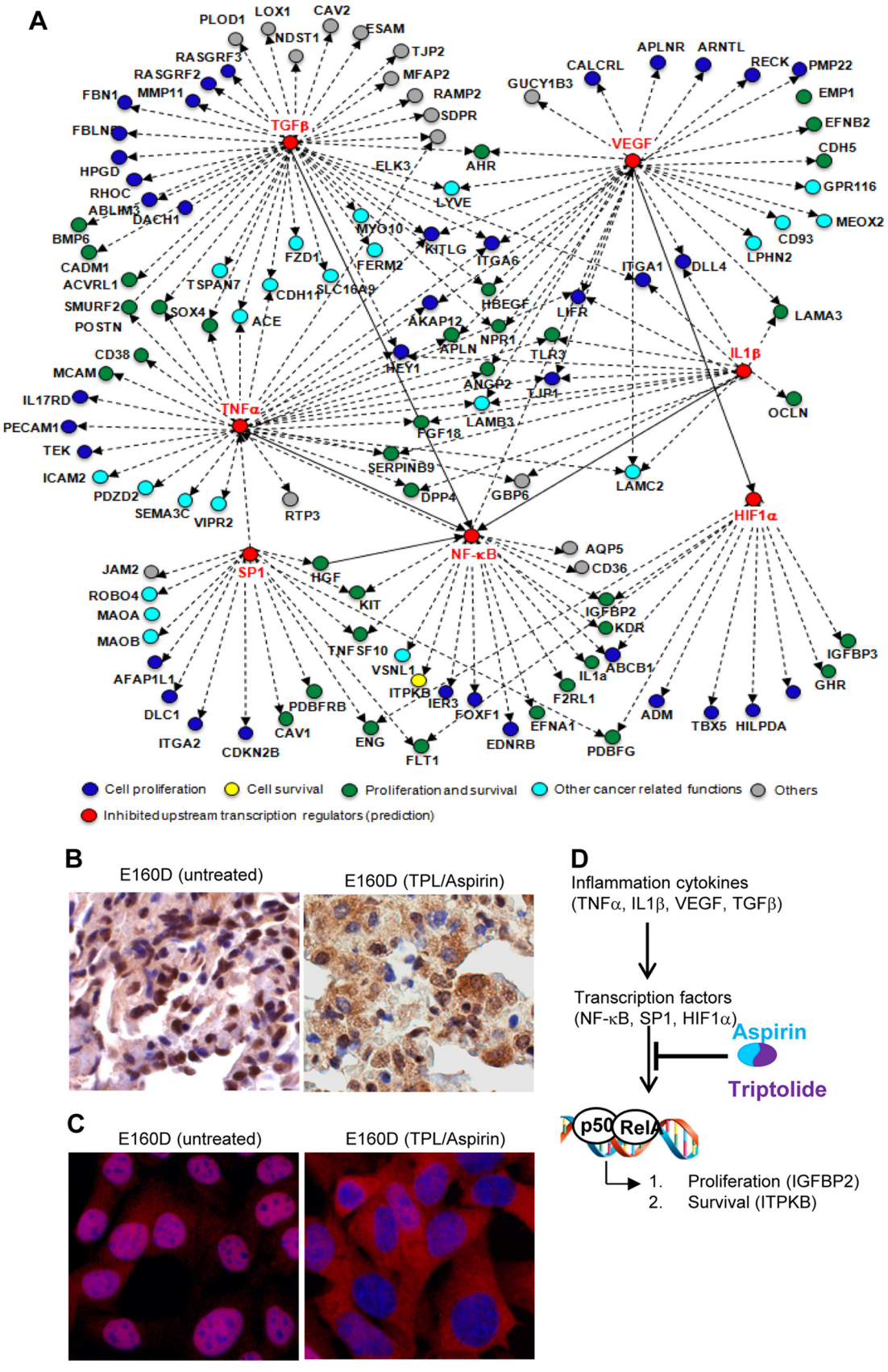

FIG 2 Low-dose triptolide and aspirin suppress NF-κB survival pathways. (A) Downregulation of inflammatory cytokine-induced genes in lung tissues of mice treated with the combination of aspirin and triptolide. Ingenuity Pathway Analysis was conducted on the microarray gene expression data to determine the molecular pathways and predicted activated and inactivated upstream

(Continued on next page)

cells, inhibited IκBα phosphorylation (Fig. 3D and F). This finding is consistent with data from a previous study implying that aspirin and salicylate are IKKβ inhibitors (17). However, triptolide, even at nonpharmacological concentrations (millimolar), did not directly inhibit IκBα phosphorylation (Fig. 3E). The addition of both triptolide and sodium salicylate to the reaction mixture did not potentiate the suppression of IκBα phosphorylation (Fig. 3F). Therefore, this indicates that triptolide does not directly inhibit IKK action or upstream factors that mediate IKK activation and instead inhibits NF-κB and potentiates the effect of aspirin through another mechanism.

This observation raises a critical question: how does triptolide inhibit NF-κB nuclear translocation and activation? We found that the inhibition of TNF-α-induced NF-κB nuclear translocation by triptolide was dependent on the status of the p53 gene. Triptolide effectively blocked TNF-α-induced NF-κB nuclear localization in cancer cells with the wild-type (WT) p53 gene, including in H460 and HeLa human cancer cells, but it had greatly reduced efficacy in blocking TNF-α-induced NF-κB nuclear localization in p53-null cancer cells, such as the H1299 and PC3 cancer cell lines (Fig. 4A to D). Furthermore, the expression of the exogenous WT p53 protein in PC3 cells restored the ability of triptolide to inhibit NF-κB nuclear localization (Fig. 4D). These findings imply that a low dose of triptolide induces a previously unknown p53-dependent mechanism for the suppression of NF-κB activation and target gene expression. Consistent with this hypothesis, we observed that triptolide treatment increased p53 protein levels at nanomolar ranges in a dose-dependent manner (Fig. 4E). On the other hand, treatment of cells with low doses of triptolide did not increase the p53 mRNA level (Fig. 4F). These findings suggested that triptolide stabilizes p53 proteins. Since p53 is also a substrate of IKKβ (18), it may compete with IκBα for substrate binding to IKKβ, thus inhibiting IκBα phosphorylation. To test this hypothesis, we used purified recombinant proteins to reconstitute ^{32}P-based IKKβ-mediated phosphorylation reaction mixtures of p53 or/and IκBα. In the reaction mixture containing p53 or IκBα as the substrate, IKKβ effectively phosphorylated p53 (Fig. 4G, lanes 1 and 2) or IκBα (Fig. 4G, lane 3). However, in the reaction mixture containing both p53 and IκBα, the level of phosphorylated p53 or IκBα was reduced (Fig. 4G, lanes 4 and 5), supporting our hypothesis that p53 and IκBα compete with each other for binding to IKKβ. In addition, we observed weak autophosphorylation of IKKβ (Fig. 4G, lane 6), but p53 or IκBα had no effect on IKKβ autophosphorylation. Western blotting further confirmed that p53 can block IKBα phosphorylation by IKKβ *in vitro* (Fig. 4H). To further test if p53 inhibited IκBα phosphorylation, we disrupted the p53 gene in WT p53-containing H460 lung cancer cells (Fig. 5A). We observed considerably higher levels of IκBα phosphorylation and ubiquitylation in p53-null H460 cells than in parent WT p53-containing H460 cells, both prior to and after TNF-α treatment (Fig. 5B). Furthermore, Western blotting and immunofluorescence staining consistently revealed that triptolide effectively inhibited TNF-α-induced IκBα phosphorylation and degradation and blocked NF-κB nuclear localization in H460 parent cells at nanomolar ranges in a dose-dependent manner, but it failed to do so in p53-null H460 cells (Fig. 5C to F). Consistently, p53-null H460 and PC3 cancer cells were more resistant to triptolide than were WT p53-containing H460 and PC3 cancer cells (Fig. 6). These findings clearly implicate a role of p53 in IκBα

FIG 2 Legend (Continued)
transcription regulators. The upstream transcription regulators are predicted by the activation *z* score (a *z* score of greater than zero is defined as activated, and a *z* score of less than zero is defined as inactivated). The top inactivated upstream transcription regulators (red nodes) and the corresponding downregulated genes (blue, yellow, green, light blue, and gray circles) for the combined aspirin-triptolide (4 mg/kg and 1 mg/kg body weight, respectively; 2-month gavage) treatment group versus the control group are shown. Solid lines indicate the activation of the transcription factor, and dotted lines indicate the induction of gene expression. (B) Representative IHC images of NF-κB in lung tissue sections of E160D mice that were untreated or treated with aspirin-triptolide (TPL). Brown, NF-κB; blue, nuclei. (C) Representative immunofluorescence staining of NF-κB in primary E160D lung adenocarcinoma cells. Cells were untreated or pretreated with aspirin or triptolide overnight and stimulated with TNF-α (10 ng/ml) for 30 min. NF-κB (red) was detected with an anti-NF-κB antibody. The nuclei (blue) were stained with DAPI. (D) Comparison of gene expression profiles in different groups of mice suggests that aspirin and triptolide potentiate each other to block proinflammatory cytokine-induced NF-κB survival pathways.

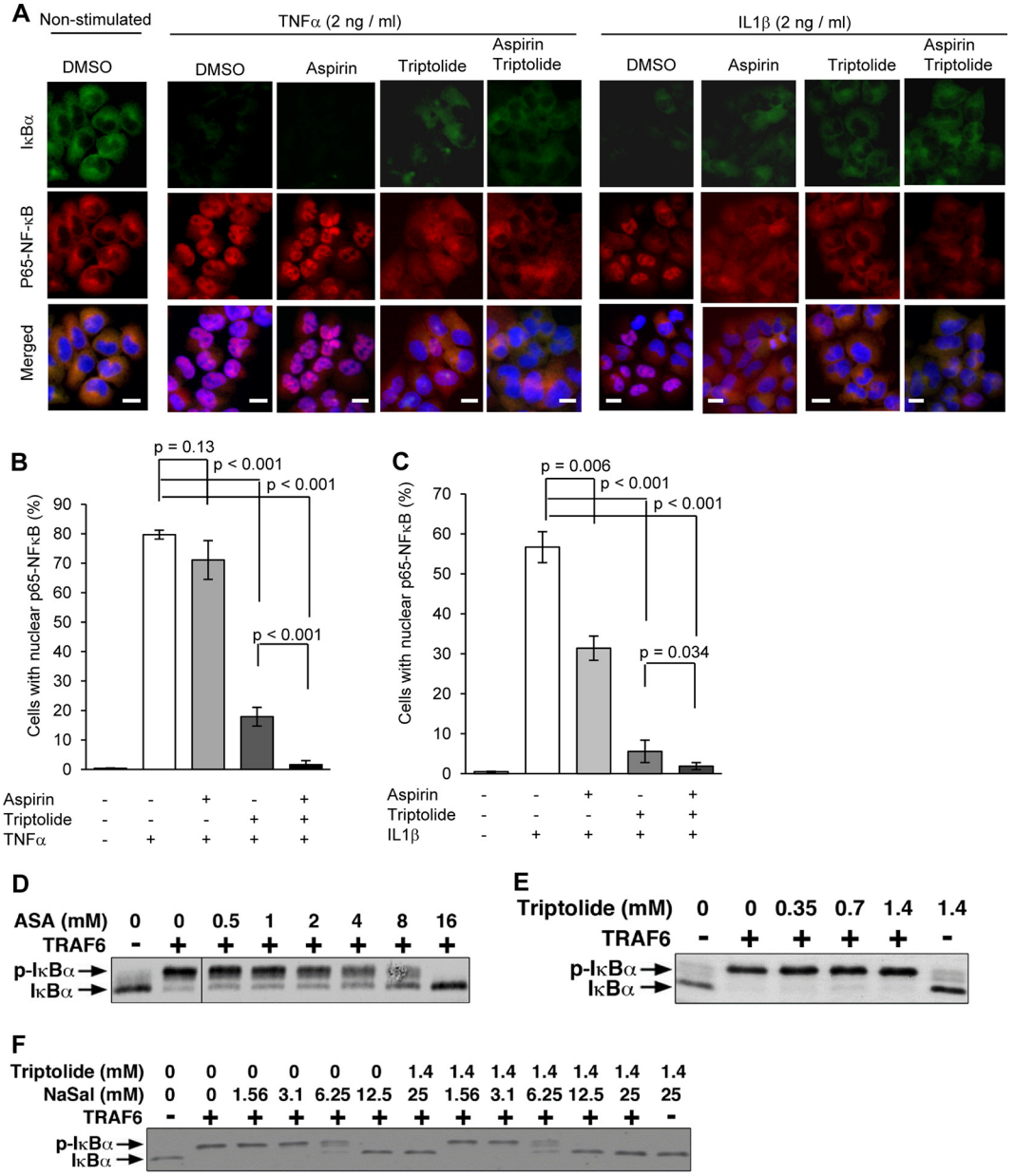

FIG 3 Triptolide and aspirin potentiate each other in inhibiting TNF-α/IL-1β-mediated NF-κB signaling. (A) TNF-α-induced IκBα degradation and NF-κB nuclear localization were examined by immunofluorescence staining. H460 cells were untreated or treated with 50 nM triptolide and/or 10 mM aspirin for 16 h. The cells were then treated with 2 ng/ml TNF-α or IL-1β for 30 min and subjected to immunofluorescence staining. Green, IκBα; red, NF-κB; blue, nucleus; pink, nuclear NF-κB. Bars, 20 μm. (B and C) Quantification of TNF-α-induced (B) and IL-1β-induced (C) NF-κB nuclear localization in H460 cells treated or not treated with aspirin and triptolide. Cells with clearly nuclear NF-κB staining were scored. Values are the means ± standard errors of the means of data from at least three independent experiments. In each experiment, more than 100 cells were analyzed. All *P* values were calculated by using two-sided Student's *t* tests. (D to F) Triptolide does not inhibit IKK activation in the cell-free system. The S100 fraction of Jurkat T cell extracts was preincubated with recombinant TRAF6 and the indicated concentrations of aspirin (ASA) (D), triptolide (E), and sodium salicylic acid (NaSal) or sodium salicylic acid and triptolide (F) for 15 min, and ATP was then added to initiate the IKBα phosphorylation reaction at 30°C for 60 min. The reaction products were then immunoblotted with anti-IκBα antibody.

phosphorylation and degradation, and by stabilizing p53, triptolide blocks the nuclear translocation of NF-κB.

Triptolide activates p38α and ERK1/2 to phosphorylate and stabilize p53 for blocking NF-κB nuclear localization. We then sought to address how triptolide induces p53 stabilization for blocking IκB phosphorylation and NF-κB nuclear localization. Because triptolide was previously found to bind to xeroderma pigmentosum type

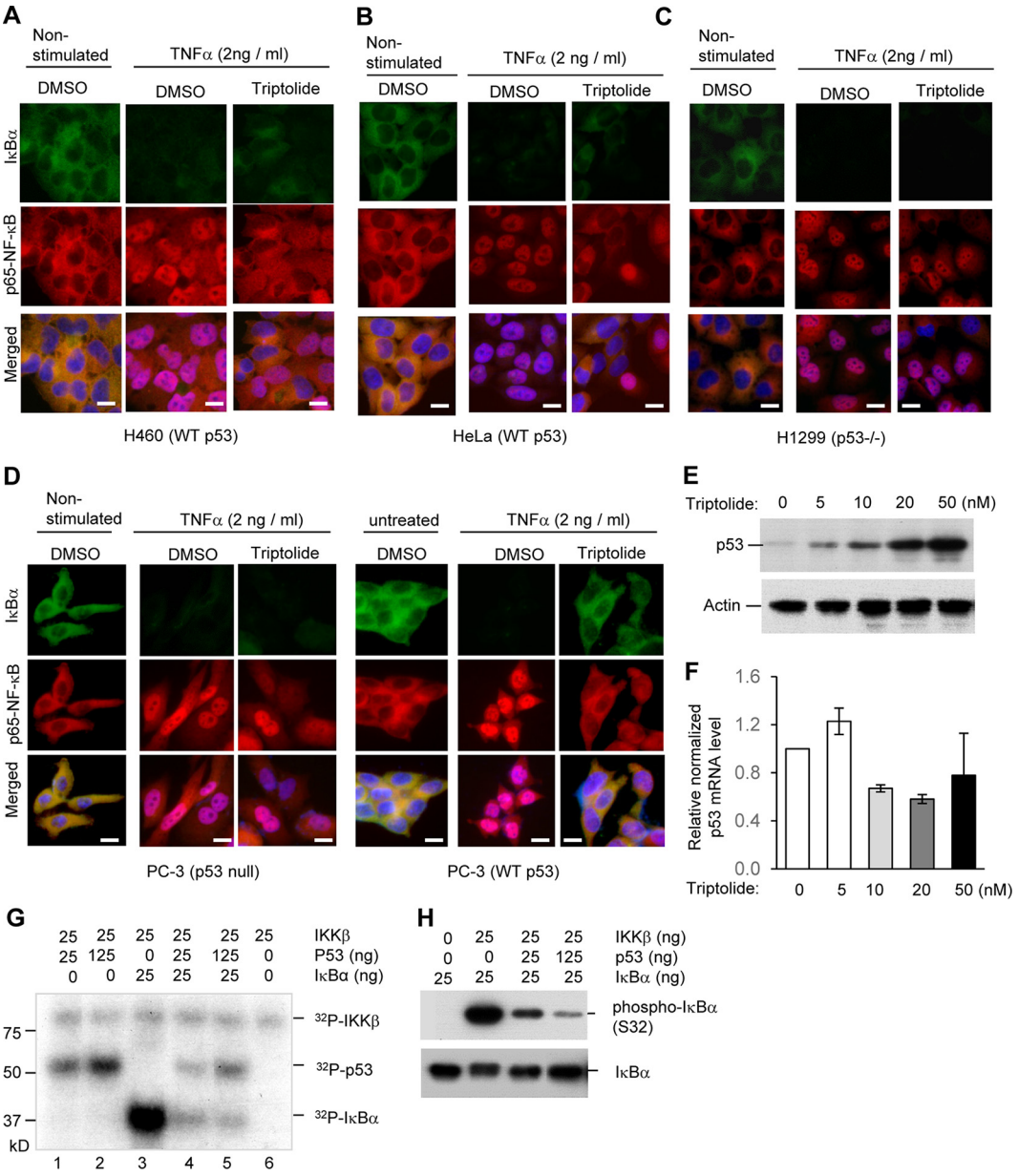

FIG 4 Effective triptolide inhibition of IκBα phosphorylation and NF-κB nuclear localization in cancer cells requires WT p53. (A to C) Triptolide impairs TNF-α-induced IκBα degradation and NF-κB nuclear translocation in H460 and HeLa (WT p53) but not H1299 (p53-null) human cancer cells. Human cancer cells were untreated or treated with 50 nM triptolide for 16 h. The cells were then stimulated with 2 ng/ml TNF-α for 30 min and subjected to immunofluorescence staining. Green, IκBα; red, NF-κB; blue, nucleus; pink, nuclear NF-κB. Bars, 20 μm. (D) Representative images of IκBα and NF-κB staining in PC3 (p53-null) cells and PC3 cells stably expressing exogenous WT p53 in response to TNF-α treatment (2 ng/ml for 30 min). Bars, 20 μm. (E) Triptolide treatment increases the p53 protein level in H460 cells in a dose-dependent manner. H460 cells were treated with 0, 5, 10, 20, and 50 nM triptolide for 24 h. Whole-cell extracts were prepared, and the p53 protein level was determined by Western blotting. (F) Quantitative PCR to measure the p53 mRNA level in H460 cells treated with 0, 5, 10, 20, and 50 nM triptolide for 24 h. The mRNA level of β-actin was used as an internal control for normalization. The normalized p53 mRNA level in the untreated control was arbitrarily set to a value of 1, and the relative p53 mRNA level in other groups was calculated by comparing the normalized p53 mRNA level to that of the control. (G) IKKβ-mediated phosphorylation of p53 and IκBα. Recombinant p53 (25 or 125 ng) and/or IκBα (25 ng) was mixed with recombinant IKKβ (25 ng) in kinase buffer containing 6.25 μM cold ATP and 0.5 μCi [^{32}P]ATP in a total volume of 10 μl. The reaction was carried out at 30°C for 30 min. The ^{32}P-labeld proteins, including p53, IκBα, IKKβ, were resolved by 8% SDS-PAGE and detected by autoradiography. (H) Reinstitution of IκBα phosphorylation by IKKβ in the absence or presence of p53. Purified recombinant IκBα (25 ng) was incubated with 0, 25, or 125 ng purified p53 in a total volume of 10 μl for 5 min on ice. The active form of recombinant IKKβ (25 ng) was then added. The reaction was carried out at 30°C for 15 min. Phosphorylated IκBα was detected by Western blot analysis. The assay was repeated at least three times.

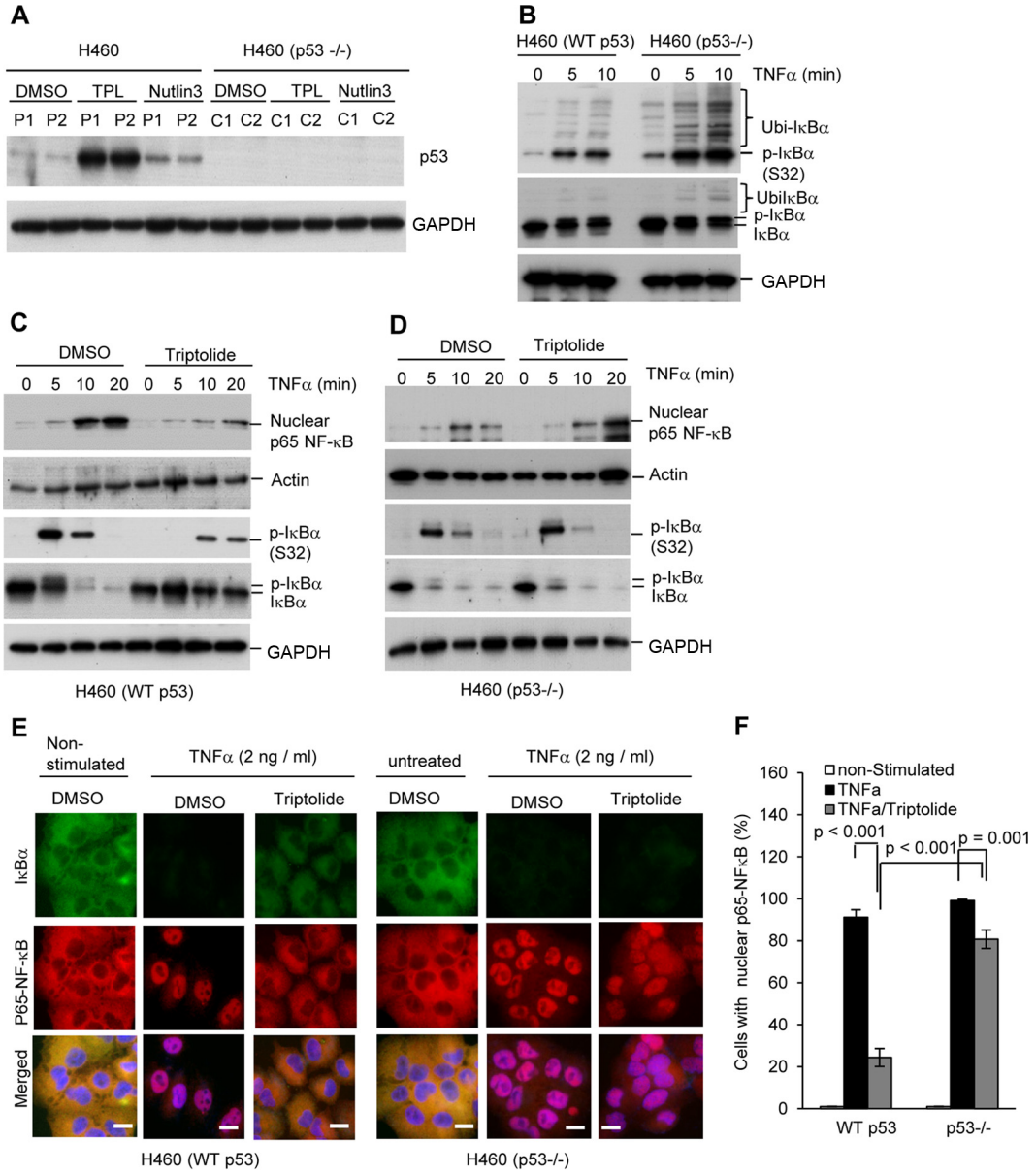

FIG 5 Knockout of p53 in H460 cells abolishes triptolide inhibition of IκBα phosphorylation and degradation and triptolide blocking of NF-κB nuclear translocation. (A) Western blot analysis to confirm p53 levels in parent and knockout H460 cells treated or not treated with triptolide (50 nM for 16 h) or nutlin3 (1 μM for 16 h). (B) IκBα phosphorylation in H460 parent and p53 knockout mutant cells in response to TNF-α. The cells were pretreated with 30 μM MG132 for 1 h, followed by stimulation of cells with TNF-α for 5 or 10 min. Whole-cell extracts were prepared, and total and phosphorylated IκBα were detected by Western blot analysis. (C and D) Western blotting showing that triptolide inhibits TNF-α-induced IκBα degradation and NF-κB nuclear translocation in H460 (WT p53) (C) but not p53-null H460 mutant (D) lung cancer cells. Parent H460 or p53-null H460 mutant cells were untreated or treated with 50 nM triptolide for 16 h. The cells were then stimulated with 10 ng/ml TNF-α for 5, 10, and 20 min. Cytoplasmic or nuclear extracts of the cells were prepared, and total phosphorylated IκBα and nuclear NF-κB were detected by Western blot analysis. GAPDH, glyceraldehyde-3-phosphate dehydrogenase. (E and F) Immunofluorescence staining showing that triptolide inhibits TNF-α-induced IκBα degradation and NF-κB nuclear translocation in H460 parent cells but not p53-null H460 mutant cells. The cells were untreated or treated with 50 nM triptolide for 16 h. The cells were then stimulated with 10 ng/ml TNF-α for 30 min and subjected to immunofluorescence staining. (E) Representative images. Green, IκBα; red, NF-κB; blue, nucleus; pink, nuclear NF-κB. Bars, 20 μm. (F) Quantification of cells with nuclear NF-κB. Values are the means ± standard errors of the means of data from at least three independent experiments. In each experiment, more than 100 cells were analyzed.

B (XPB), which is a subunit of RNA polymerase II, and to play an important role in transcription and nucleotide excision repair (19); a possible mechanism is to induce DNA damage and activate ATR, which was previously shown to phosphorylate p53 at the S37 residue and stabilize p53 (20). We observed that a low dose of triptolide

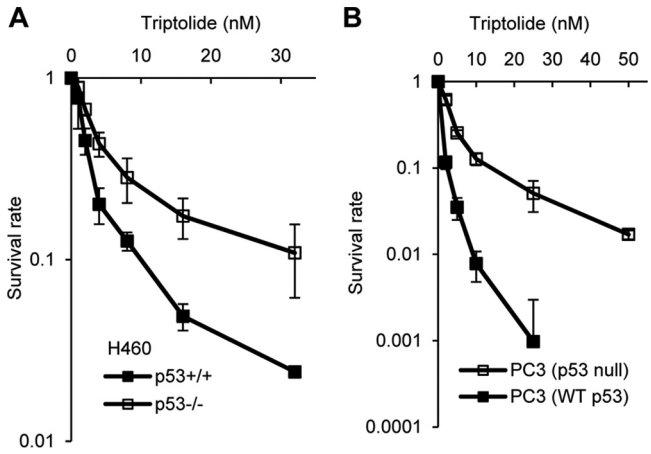

FIG 6 p53 is critical for triptolide to suppress proliferation and survival of cancer cells. (A) Survival rates of H460 (WT p53) and H460 (p53-null) lung cancer cells in the absence or presence of different concentrations of triptolide. (B) Survival rates of PC3 (p53-null) and PC3 prostate cancer cells complemented with exogenous WT p53 in the absence or presence of different concentrations of triptolide. In both panels, live cells were counted after 4 days of incubation in DMEM with or without the indicated concentrations of triptolide. The survival rate of untreated cells was arbitrarily set to a value of 1. The survival rate of other cells treated with triptolide was calculated by comparing the total number of live cells to that of the untreated controls. Experiments were repeated three times independently. Values are means ± standard deviations.

induced γH2AX foci, an indicator of DNA damage, in approximately 30% of the cells (Fig. 7A). However, triptolide caused p53 stabilization in all cells (Fig. 7A). In addition, the knockdown of ATR in H460 cells did not considerably abolish triptolide-induced p53 stabilization (data not shown). Thus, while low-dose triptolide-induced DNA damage contributes to p53 stabilization, there must be a new mechanism that plays the primary role in p53 phosphorylation and stabilization. To identify new target proteins of triptolide and to reveal the mechanism by which triptolide causes p53 stabilization, we employed the ligand-protein inverse docking (INVDOCK) strategy to screen the Brookhaven Protein Data Bank (PDB). We found that triptolide binds to a wide spectrum of transferases, including kinases, nucleotide binding proteins and modifiers, and acetyltransferases. Of these potential targets, the tyrosine kinases and serine/threonine/protein kinases (STKs) (Pfam accession number PF00069) were highly enriched ($P = 0.0023$), including MAPK14 (p38α) (Fig. 7B). Further molecular docking analysis suggested that triptolide binds at a site near the highly conserved ATP pocket of the kinase domain of p38α or the other STKs (Fig. 7C, top). The model structure of triptolide binding to the p38α-ATP complex showed that triptolide can form hydrogen bonds with the T106 residue in the ATP binding pocket of p38α, resulting in a stable triptolide-p38α-ATP complex (Fig. 7C, bottom).

The molecular docking results suggested that triptolide might bind to kinases and modulate their activities. We then determined the impact of triptolide on kinases in H460 cells using the Phosphor Explorer array, which evaluates the protein levels of kinases and the corresponding phosphorylated substrates. We found that in triptolide-treated H460 cells, the levels of the kinases p38α (MAPK14), CSNK2A1, IGF1R, glycogen synthase kinase 3β (GSK3β), and FAK1, which were identified as potential triptolide targets by INVDOCK, were considerably increased (>2-fold) compared to those in untreated controls (Fig. 7D). It is unclear how triptolide binding would affect the overall protein levels of these kinases. One possibility is that the binding of triptolide to kinases enhances their stabilities. In further support of a kinase-mediated mechanism of triptolide action, the levels of a number of phosphorylated proteins, including p53, which are the substrates of these kinases, including p38α and ERK1/2, were increased in triptolide-treated H460 cells (Fig. 7E).

These data suggested that triptolide might activate p38α and ERK1/2 to phosphorylate p53 for its stabilization. The phosphorylation of p53 at N-terminal serine residues

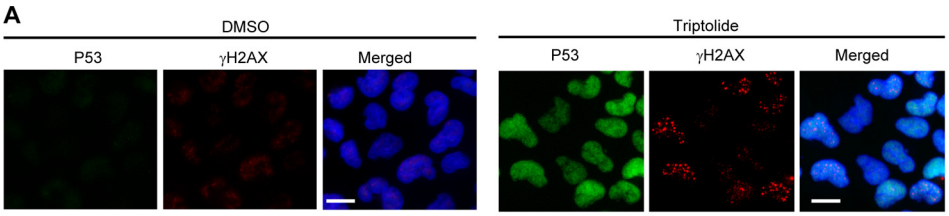

B

Top potential protein targets of triptolide searched by INVDOCK

PDB ID	Protein Name	Activity	Docking score
2C6I	CDK2	kinase	-47.5
1BG2	KIF5B	ATPase	-47.5
1OEC	FGFR2	kinase	-46.3
1XJD	PRKCQ (PKCδ)	kinase	-45.3
2GFS	MAPK14 (p38α)	kinase	-43.4
1BYG	CSK (c-SRC)	kinase	-42.8
1UOU	TYMP	phosphorylase	-41.9
2PVR	CSNK2A1	kinase	-41.3
2ETM	FAK1	kinase	-41.1
1J1B	GSK3β	kinase	-40.6
2OJ9	IGF1R	kinase	-39.2

C

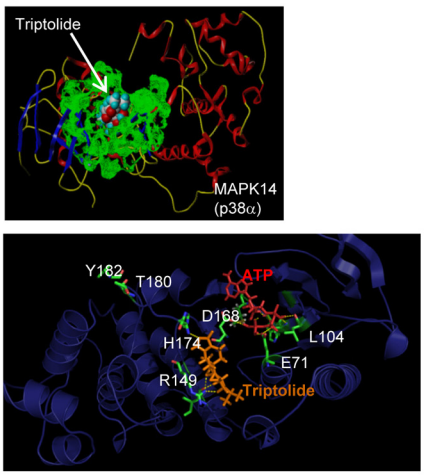

D

Activated kinases in triptolide-treated H460 cells

Protein Name	Relative protein level	Enhanced Phospho-substrates
MAPK1/3 (ERK1/2)	2.2	16
MAPK14 (p38α)	2.0	9
CSNK2A1	3.2	6
PRKCA(PKCα)	3.3	4
IGF1R	2.1	4
GSK3β	3.7	2
FAK1	3.3	1

E

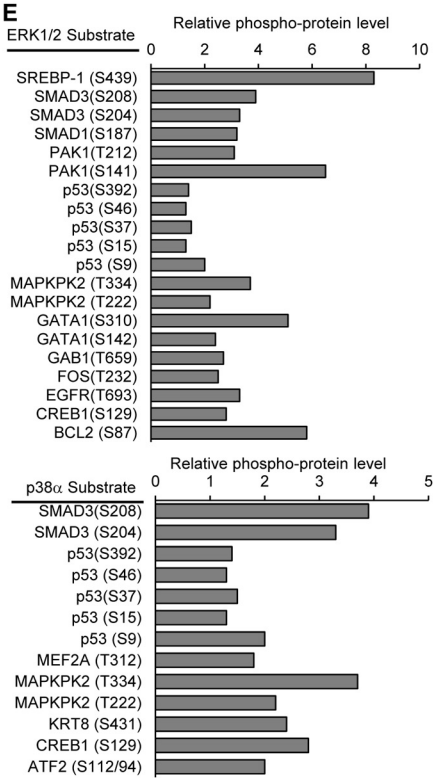

FIG 7 Triptolide stabilizes and activates p38α and ERK1/2 kinases. (A) Triptolide induces γH2AX DNA damage foci in a subset of cells but p53 stabilization in all cells. H460 cells were treated or not treated with triptolide (50 nM for 16 h) and costained with antibodies against p53 and γH2AX (S139). Red, γH2AX (S139); green, p53; blue, nucleus. Bars, 20 μm. (B) List of the top potential targets of triptolide searched by INVDOCK. CDK2, cyclin-dependent kinase 2. (C) Molecular docking of triptolide to MAPK14 (p38α) (PDB accession number 2GFS). (Top) Overall docking structure. The green area shows the surface of the active site of p38α. The space-filling model molecule is triptolide. (Bottom) Detailed model structure of triptolide binding to the p38α-ATP complex. Blue, backbone structure of p38α; orange, triptolide molecule; red, ATP molecule; green, key residues that coordinate with triptolide or ATP. The hydrogen bond is indicated by the dotted yellow line. (D and E) Effects of triptolide on kinase signaling. The levels of kinases and the corresponding phosphorylated protein substrates in total cell extracts from H460 cells that were untreated or treated with triptolide (50 nM for 16 h) were measured by an antibody array. The protein level for the untreated control was arbitrarily set to a value of 1. Values are the averages of data from two arrays. A phosphorylated protein substrate with a relative level of >2 in triptolide-treated cell extracts was scored as a triptolide-enhanced phospho-substrate. (D) Kinases with a relative level of >2 and at least one corresponding enhanced phospho-substrate in triptolide-treated H460 cell extracts. Red indicates the kinases identified by both INVDOCK and antibody array analyses. (E) Relative levels of phosphorylated protein substrates of ERK1/2 or p38α in triptolide-treated H460 cell extracts.

was previously shown to disrupt its interaction with the E3 ubiquitin ligase MDM2, which mediates p53 degradation and stabilizes the p53 protein (21). In addition, p53 phosphorylation has been shown to be critical for inducing its oligomerization, stabilization, and nuclear localization (22). Previous studies demonstrated that p38α directly phosphorylates p53 or activates PRAK to catalyze p53 phosphorylation at the S37 residue (23, 24). ERK1/2 has been shown to phosphorylate and activate p53 in response to many stress conditions (23). Supporting our hypothesis, we revealed that triptolide induced the phosphorylation and activation of p38α and ERK1/2 (Fig. 8A and B), and the activation of these two kinases coincided with p53 stabilization (Fig. 8A). To test if p38α and/or ERK1/2 mediates p53 phosphorylation/stabilization, we pretreated H460 cells with the p38α inhibitor SB203580 (25) and the MEK inhibitor U0126 (26), which blocks ERK1/2 phosphorylation and activation. We found that either SB203580 or U0126 alone partially blocked triptolide-induced p53 phosphorylation and stabilization in H460 cells (Fig. 8C and D). However, the combination of both drugs blocked p53 phosphorylation and stabilization in more than 95% of H460 cells (Fig. 8C and D). Furthermore, we found that the p53 Ser37A mutant, which abolishes p53 phosphorylation, failed to be stabilized by triptolide in cells (Fig. 8E). These findings support the hypothesis that triptolide activates p38α and ERK1/2 to phosphorylate and stabilize p53. Next, we addressed if p38α- and ERK1/2-mediated p53 Ser37 phosphorylation and stabilization are critical for triptolide to block NF-κB nuclear localization. We observed that the addition of SB203580 and U0126 abolished the effects of triptolide on blocking the nuclear localization of NF-κB (Fig. 8F). Similarly, the p53 Ser37A mutation also resulted in an abolishment of the inhibitory effect of triptolide on NF-κB nuclear translocation (Fig. 8G). These results suggest that p38α and ERK1/2 are likely to be the direct intracellular targets of triptolide, leading to p53 phosphorylation and stabilization, decreased NF-κB nuclear localization, and decreased cell proliferation.

DISCUSSION

We present a promising regimen for the prevention and treatment of inflammation-associated cancers such as lung cancer, which is the leading cause of cancer deaths worldwide. Effective therapies to improve survival are needed (27). A potentially important strategy to reduce lung cancer-related mortality is to prevent lung cancer from developing in high-risk populations or to reduce its recurrence after treatment of early-stage cancer. Because of the causal role of chronic inflammation in lung cancer development (28, 29), anti-inflammatory molecules have been tested for chemoprevention of lung cancer (30, 31). However, effective strategies for the prevention and treatment of lung cancer remain to be developed. In particular, NF-κB has proven to be a promising drug target, but prior anti-NF-κB therapies have not been successful due to off-target effects and toxicity. Aspirin and triptolide were previously found to inhibit NF-κB activity. Aspirin has been tested in clinical trials as a chemoprevention agent for colon and breast cancers (32–34). In this study, we discovered that within a low dosage range, the anti-inflammatory molecules aspirin and triptolide individually only moderately inhibited lung cancer development in mice. However, the strategy of combining low doses of aspirin and triptolide is promising, as this combination displays strong potentiation and high efficacy. Therefore, this suggests that the combined administration of low doses of anti-inflammatory drugs is a feasible and effective way to prevent lung cancer. Similar strategies may also be applied to the chemoprevention of other inflammation-associated cancers such as colon cancer and prostate cancer. Because triptolide can simultaneously activate p53 and inhibit NF-κB, it has the potential to treat human cancer. Indeed, triptolide has been shown to inhibit pancreatic cancer cell survival and tumor formation in mice (13, 15). It is currently in clinical trials for pancreatic cancer treatment. Our study suggests that triptolide may be an effective chemotherapeutic agent for the treatment of lung cancer, while aspirin may potentiate triptolide's efficacy. In addition, we consider that the activation of p53 signaling and blocking of NF-κB-mediated survival pathways by triptolide may also sensitize lung

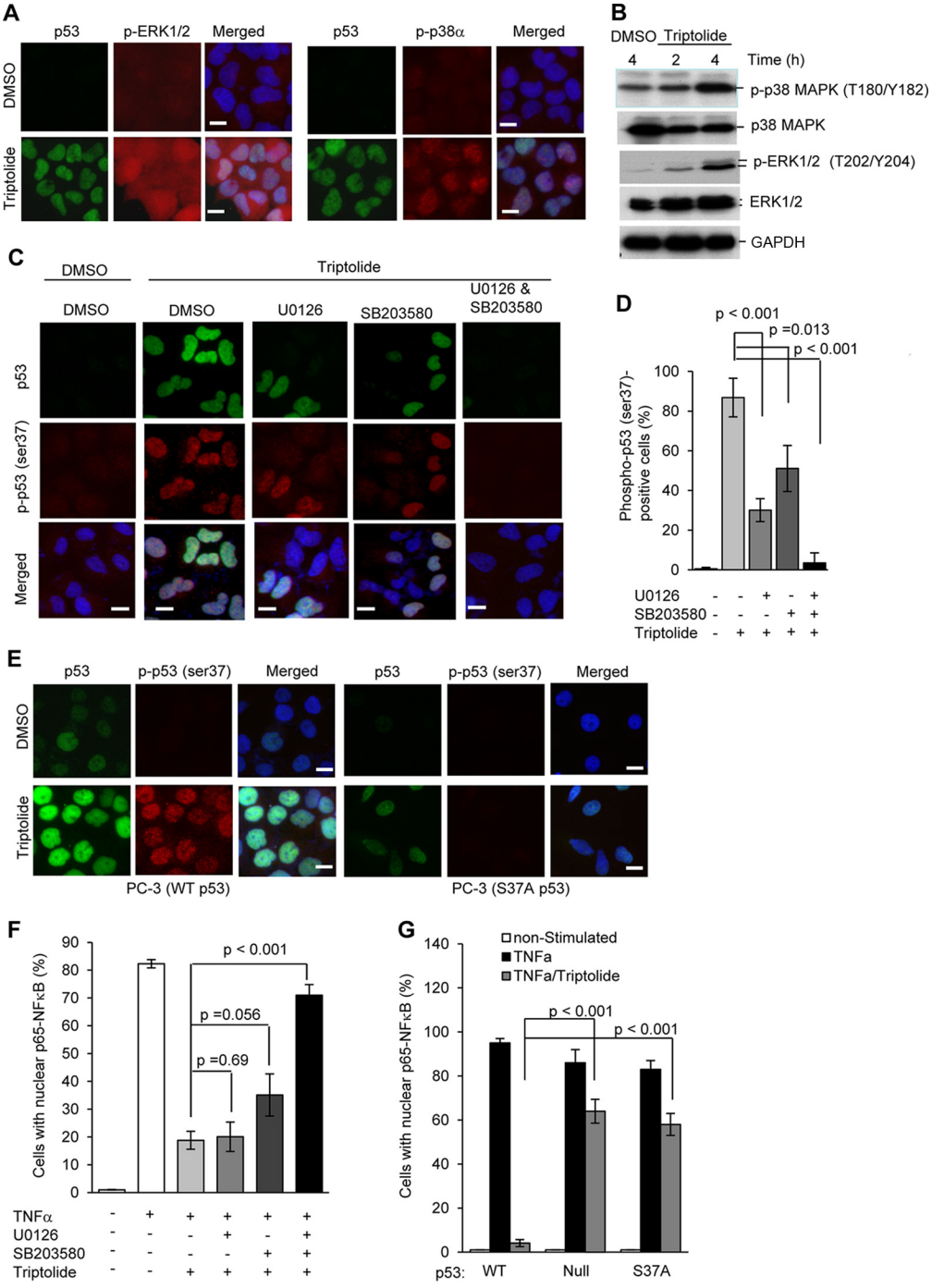

FIG 8 ERK1/2- and p38α-mediated p53 phosphorylation and stabilization are responsible for triptolide inhibition of NF-κB nuclear localization. (A) Coimmunofluorescence of phosphorylated ERK1/2 (T202/Y204)/p53 and phosphorylated p38α (T180/Y182)/p53 in H460 cells treated with triptolide (0 or 50 nM for 16 h). Red, phosphorylated ERK1/2; green, p53; blue, nucleus. (B) Western blotting of phosphorylated ERK1/2 and p38α in H460 cells treated with triptolide (0 or 500 nM for 2 or 4 h). (C and D) H460 cells were pretreated with the MEK inhibitor U0126 (10 μM), the p38α inhibitor SB203580 (10 μM), or both for 2 h and treated with 20 nM triptolide for 16 h. (C) Representative immunofluorescence staining images of p53 (green) and phosphorylated p53 (S37) (red) in H460 cells. (D) Quantification of phosphorylated p53-positive cells. (E) The Ser37A p53 mutation abolishes triptolide-induced p53 stabilization. Shown is costaining of total p53 and phosphorylated p53 (S37) in PC3 cells stably expressing exogenous WT or S37A p53 proteins. Red, phosphorylated p53; green, p53; blue, nucleus. (F) Inhibition of p38α and ERK1/2 abolishes triptolide's function to block NF-κB nuclear localization. H460 cells that were treated with drugs, as indicated in panels C and D, were stimulated with TNF-α (2 ng/ml for 30 min) and nuclear NF-κB and detected by immunofluorescence. The number of cells with clear nuclear NF-κB was quantified. (G) Nuclear NF-κB staining in TNF-α-untreated and treated PC3 cells stably expressing exogenous WT or S37A p53 proteins. The number of cells with clear nuclear NF-κB was quantified. In both panels F and G, values are the means ± standard errors of the means of data from at least three independent experiments, each using >100 cells. All *P* values were calculated by using two-sided Student's *t* tests.

cancer cells to conventional chemotherapy such as cisplatin and paclitaxel. Thus, it may be used as an adjuvant component for conventional chemotherapy.

Our study further defines the mechanisms by which aspirin and triptolide effectively suppress cancer development. It is known that the initiation of cancer cells results in oncogenic stress, leading to DNA damage responses, the activation of cell cycle checkpoint regulators such as p53, and, subsequently, senescence and apoptosis (35, 36). Cancer cells at least partly depend on the expression of cellular survival genes to counteract oncogenic stress, and the expression of these survival genes is controlled by transcription factors such as NF-κB (37, 38). NF-κB activation has been shown to be a key molecular event during the development of chronic inflammation-associated cancer (7–9). We show that aspirin and triptolide effectively block p65/NF-κB nuclear translocation in response to inflammatory cytokines, reduce the levels of total and phosphorylated p65/NF-κB, and consequently shut down a major linkage between chronic inflammation and cancer development. First, by blocking NF-κB, aspirin and triptolide together suppress proinflammatory TGF-β-, IL-1β-, TNF-α-, and VEGF-mediated cytokine signaling pathways in lung tissues. Consequently, these anti-inflammatory drugs inhibit the expression of genes controlling cell viability, proliferation, and angiogenesis, which are critical for promoting tumor growth. Second, aspirin and triptolide suppress the NF-κB-mediated expression of antiapoptosis proteins such as survivin in cancer cells, thus disrupting an important mechanism for the cells to escape apoptosis. Furthermore, the activation of p53 and the upregulation of its target genes, such as p21, may also contribute to the effects of aspirin-triptolide on cancer suppression.

Triptolide was previously implicated as an inhibitor of NF-κB (39–41), but the underlying molecular mechanism remains unclear. Our present study has defined the molecular mechanism by which triptolide inhibits NF-κB, and aspirin greatly potentiates this inhibitory effect (Fig. 9). We show that triptolide, at nanomolar concentrations, effectively inhibits IκBα degradation and NF-κB nuclear translocation. However, triptolide does not directly act on the processes of IκBα phosphorylation and NF-κB nuclear translocation. Instead, it executes its inhibitory function on NF-κB via p53. We have revealed that triptolide indeed activates p38α and the ERK1/2 kinases to phosphorylate p53, which subsequently results in the stabilization of p53 (Fig. 9). The requirement for phosphorylated p53 in triptolide action is demonstrated by the fact that the abolishment of p53 phosphorylation by ERK1/2 and p38α inhibitors allows TNF-α-induced NF-κB nuclear translocation in the presence of triptolide. In addition, both triptolide-activated ERK1/2 and p38α are likely to be important, because the blocking of either kinase only partially restores TNF-α-induced NF-κB nuclear translocation. The molecular mechanism revealed in our study explains a previously reported observation that triptolide inhibition of NF-κB transcription activity required a functional p53 gene (40). In addition, the observation that triptolide inhibits NF-κB action in a p53-dependent manner is consistent with data from previous studies indicating that p53 may affect NF-κB activity (42) and that mutated p53 is linked to aberrant NF-κB activation, which contributes to inflammation-associated colon cancer (43). Furthermore, aspirin, which was originally found to modify and inactivate the inflammation mediator Cox-2 (44), has also been shown to directly inhibit IKKβ activity and the subsequent activation of NF-κB (17). Altogether, by directly inhibiting IKKβ activity, which mediates IκBα phosphorylation and degradation, and by inducing the p53-dependent stabilization of IκBα, the combined use of low-dose aspirin-triptolide effectively inhibits the nuclear translocation of NF-κB in response to proinflammatory cytokines and blocks the inflammation-promoted proliferation and survival of cancer cells.

Our data also shed light on the molecular targets of triptolide and at least partly explain the multiple biological activities of this potent anti-inflammatory and anticancer compound. Results from our comprehensive screening for triptolide targets by the INVDOCK strategy reveal that triptolide potentially binds to various proteins that contain an ATP binding motif. Further structural analysis of the triptolide-p38α kinase complex indicates that triptolide binds to the active site of p38α, near the ATP binding

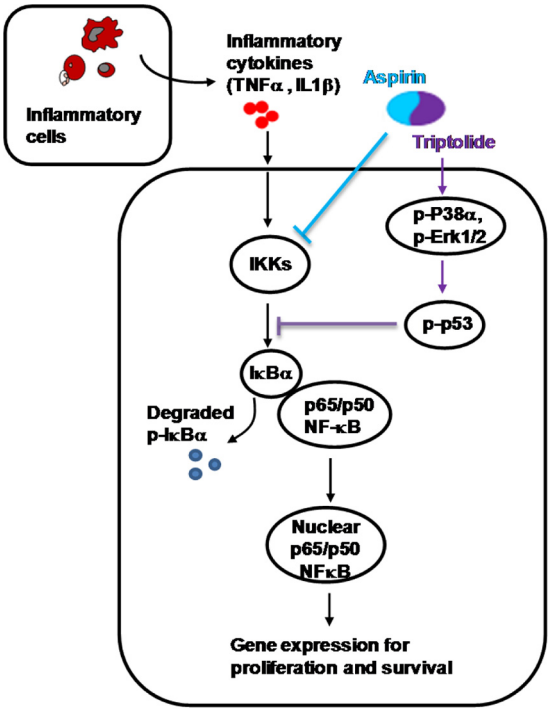

FIG 9 Schematic graph elucidating the therapeutic targets of aspirin and triptolide for chemoprevention of inflammation-associated lung cancer and other cancers. Inflammatory cytokines such as TNF-α, IL-1α, and IL-1β bind to their receptors to activate the IKK complex, which phosphorylates IκBα, the inhibitory subunit of NF-κB. Degradation of phosphorylated IκBα results in the nuclear translocation of p65 NF-κB and the induction of the gene expression of cell proliferation and survival genes. However, aspirin directly inhibits the phosphorylation of IκBα by the IKK complex, and triptolide activates p38α and ERK1/2 to phosphorylate and stabilize p53, which also blocks the phosphorylation of IκBα by the IKK complex. Together, triptolide and aspirin effectively block inflammation-induced NF-κB-mediated proliferation and survival signaling.

site, without competing with ATP for binding to p38α. The binding of a small molecule to the ATP binding pocket of kinases could modulate kinase activity as an agonist or an antagonist (for a recent review, see reference 45). Our biochemical data suggest that triptolide stabilizes the kinase targets identified by INVDOCK and phosphorylates the downstream protein substrates. However, triptolide may also work as an inhibitor of kinases, ATPases, or other transferases. A recent study suggests that the binding of triptolide to the TAB1/TAK1 complex inhibits its kinase activity (46). Another study shows that triptolide binds to XPB, inhibits its ATPase activity, and subsequently suppresses *de novo* RNA synthesis and nucleotide excision repair (19). Our molecular docking data showing that triptolide may bind to acetyltransferases also support the previous finding that triptolide can act as an acetyltransferase inhibitor (47). Thus, triptolide can potentially bind to a wide spectrum of proteins that contain ATP binding motifs and change their enzymatic activities; this explains why triptolide is able to affect many cellular processes and have potent cytotoxicity. Nevertheless, at low concentrations, triptolide may primarily bind to the high-affinity target to activate p38α, ERK1/2, and, subsequently, p53 to block NF-κB activation. Therefore, by combining triptolide with aspirin and its derivatives, we have identified a candidate anticancer regimen that uses low therapeutic doses and may bypass the safety and efficacy problems that are typically associated with high-dose single-agent therapies. This novel therapeutic strategy could greatly improve the prevention and treatment of inflammation-associated cancers.

MATERIALS AND METHODS

Animal studies. FEN1 E160D mice (129S1 genetic background), which are prone to developing inflammation-associated lung cancer, were in-line bred and housed in the Animal Resource Center at City

of Hope. All experimental protocols involving animals were approved by the Research Animal Care and Use Committee of City of Hope in compliance with Public Health Service policies of the United States and China and all other federal, state, and local regulations. To test the efficacy of aspirin and triptolide in suppressing lung cancer development, E160D mice (10-month-old males and females; $n = 30$ for each group) were randomly divided into untreated, aspirin-treated (4 mg/kg body weight), triptolide-treated (1 mg/kg body weight), and aspirin (4 mg/kg body weight)-triptolide (1 mg/kg body weight)-treated groups. Aspirin was purchased from Sigma (St. Louis, MO), and pharmaceutical-grade triptolide was purchased from Shanghai Fudan Fuhua Pharmaceuticals Ltd. (Shanghai, China). The aspirin solution and/or the triptolide suspension was administered to mice by gavage 5 days a week for 2 months. After an additional 4 months, the mice were euthanized and subjected to anatomic analysis to assess abnormalities, including tumor formation in major organs. Lung adenomas and adenocarcinomas were analyzed by routine histopathology analysis at the Department of Pathology at City of Hope in a blind fashion. For the mouse Lewis lung carcinoma-grafted mouse model, 1.0×10^6 mouse Lewis lung carcinoma cells were subcutaneously injected into WT mice (8 weeks old). The mice were randomly divided into a control and three treatment groups ($n = 10$ for each group). From the third day postgrafting, the mice were administered an aspirin solution (4 mg/kg body weight) and/or a triptolide suspension (1 mg/kg body weight) by gavage for 4 weeks. From the second week post-tumor grafting, the tumor size for each mouse was measured by using the ellipsoid volume formula ($1/2 \times$ height $\times$ width $\times$ length) (48). At the end of the experiment, the tumors were dissected and weighed.

Cell culture, drug treatment, and cell proliferation assays. Cancer cells, if not otherwise specified, were cultured in Dulbecco's modified Eagle's medium (DMEM) supplemented with 10% fetal bovine serum (FBS) and 1% penicillin-streptomycin. PC3 cancer cells were cultured in RPMI 1640 supplemented with 10% FBS and 1% penicillin-streptomycin. For drug treatments, triptolide (Lingonberry Group, Hei Long Jiang, China) (purity of >98% as determined by high-performance liquid chromatography [HPLC]), aspirin and sodium salicylate (Sigma, St. Louis, MO) (purity of >99%), U0126 (Cell Signaling Technology, Danvers, MA) (purity of >99%), or SB203580 (Santa Cruz Biotechnologies, Santa Cruz, CA) (purity of >98%) was dissolved in dimethyl sulfoxide (DMSO) and diluted in DMEM or RPMI 1640 to a specific concentration, and the pH value of the medium was adjusted. Cells were incubated with medium containing the drugs for the indicated times and further processed. The cell proliferation rate was analyzed as described previously (49, 50). Briefly, H460, H460 p53 knockout, or PC3 cancer cells were seeded onto 6-cm dishes. The cells were grown in medium at 37°C and counted by using a hemacytometer every day for 4 days. The cell proliferation rate is expressed as the increase in the cell number in a given time period.

Establishment of p53-null H460 mutant cells by CRISPR. Clustered regularly interspaced short palindromic repeat (CRISPR) oligonucleotides (forward primer CACCGAGGGAAGCGTGTCACCGTCG and reverse primer AAACCGACGGTGACACGCTTCCCTC) were designed by using the CRISPR design tool (http://crispr.mit.edu/) and subcloned into the pSpCas9(BB)-2A-Puro(pX459) CRISPR gene targeting vector (51). The vector was transfected into H460 cells, which were briefly selected with puromycin (1 μg/ml) for 24 h. The selected clones were expanded and verified for the p53 homozygous knockout by Western blot analysis.

Microarray gene expression analysis. For microarray analysis, E160D mice were untreated or treated with aspirin and/or triptolide for 2 months and immediately euthanized. Total RNA was extracted from the lung tissues isolated from age-matched untreated, aspirin-treated, triptolide-treated, or aspirin-triptolide-treated E160D mice ($n = 3$ for each group) by using the Qiagen RNeasy kit (Qiagen). The GeneChip mouse gene 1.0-ST array (Affymetrix, Santa Clara, CA) was used to define gene expression profiles from the samples. Synthesis and labeling of cDNA targets and hybridization and scanning of GeneChips were carried out by the Integrative Genomics Core Facility at City of Hope according to protocols that we described previously (36). Raw intensity measurements of all probe sets were background corrected, normalized, and converted into expression measurements by using Affymetrix expression console v1.1.1. The Bioconductor "LIMMA" package was then used to identify genes differentially expressed between the drug-treated and untreated (control) E160D mouse groups. Genes with significantly different expression levels were selected by using a cutoff of a P value of <0.05 and a fold change of >1.5. Ingenuity Pathway Analysis was used to identify the pathways and upstream transcription regulators of the groups of genes that were upregulated or downregulated. A pathway or an upstream transcription regulator is defined as activated if its activation z score is greater than zero and as inactivated if its z score is less than zero.

***In vitro* assay of cell-free TAK1-IKK activation.** A cell-free *in vitro* TRAF6-based TAK1-IKK activation assay was performed according to previously reported protocols (16). Briefly, total cellular proteins were extracted from Jurkat T cells, and the supernatant was collected after centrifugation at 100,000 $\times$ g for 1 h at 4°C (termed S100). To analyze the effects of aspirin, sodium salicylate, or triptolide, the S100 cell extract (10 to 15 μg total protein) and purified recombinant TRAF6 (120 ng) were incubated with various concentrations of these chemicals in a total volume of 10 μl in reaction buffer (50 mM Tris-Cl [pH 7.4], 5 mM $MgCl_2$, 0.5 mM dithiothreitol [DTT]). The mixture was incubated on ice for 15 min, and ATP (final concentration, 2 mM) was then added to initiate the reaction. After further incubation at 30°C for 1 h, the reaction was stopped by the addition of 5$\times$ SDS sample buffer and boiling at 95°C for 5 min. The reaction products were separated by 10% SDS-PAGE and immunoblotted by using antibodies against IκBα (Cell Signaling Technologies).

Reconstitution of IκBα phosphorylation by IKKβ. Purified recombinant IκBα (Sino Biological Inc.) was preincubated with purified recombinant p53 (R&D Systems) in the presence of reaction buffer (50 mM Tris-Cl [pH 7.4], 5 mM $MgCl_2$, 0.5 mM DTT, 2 mM ATP). Recombinant IKKβ (EMD Millipore) was added

to the mixture to initiate the kinase reaction. In the kinase assay using [^{32}P]ATP, a mixture of 5 μM cold ATP and 0.5 μCi [^{32}P]ATP rather than 2 mM ATP was used. After incubation at 30°C for a specific time, the reaction was stopped by the addition of 2× SDS sample buffer and boiling at 95°C for 5 min. The reaction products were separated by 10% SDS-PAGE and immunoblotted by using antibodies against IκBα and phospho-IκBα (S32) (Cell Signaling Technologies).

Immunofluorescence staining. For the NF-κB nuclear localization assays, cells (on coverslips) with or without various pretreatments with aspirin, sodium salicylate, triptolide, U0126, and/or SB203580 for 14 h were stimulated with TNF-α, IL-1α, or IL-1β for 30 min. To costain for IκBα and NF-κB, the cells were fixed with 4% paraformaldehyde, permeabilized with 0.1% Triton X-100, blocked with the Image iT FX signal enhancer (Invitrogen), and incubated (1.5 h at room temperature) with the indicated primary antibodies. Antibodies against IκBα (1:100) and NF-κB (1:200) were obtained from Cell Signaling Technology. The cells were then washed with phosphate-buffered saline (PBS) and incubated (1 h at room temperature) with the corresponding secondary antibodies (1:200; Invitrogen). The slides were washed with PBS, counterstained with 4′,6-diamidino-2-phenylindole (DAPI), and analyzed with a fluorescence microscope (AX70; Olympus). The same immunofluorescence staining protocol was used to detect p53 or phosphorylated p53 at different sites, phosphorylated p38α (T180/Y182), and phosphorylated ERK (T202/Y204) in cells with different treatments. All these antibodies were obtained from Cell Signaling Technology and were used at a 1:200 dilution.

Virtual screening of triptolide targets by INVDOCK and pathway enrichment analysis. The potential protein targets of triptolide were computationally screened against a Brookhaven PDB-derived protein cavity database by INVDOCK, an inverse docking tool developed previously by Chen and Zhi (52). In the present study, the search was limited to protein entries derived from mammals. Triptolide was docked to sites inside each protein cavity, starting from known ligand binding sites of the protein. The other interior sections of proteins would be used if triptolide failed to dock with known ligand binding sites. To save central processing unit (CPU) time, the program was designed to search for and record the first successful dock within each cavity. To avoid redundancies, all cavity entries were subjected to screening unless the related proteins had been identified as potential targets. Finally, we considered proteins with crystal structures of a ≤2.5-Å resolution, which is a measure of the quality of the crystal structure. To reduce the false-positive prediction rate from this method, the docking results for triptolide were refined by domain and pathway enrichment analyses. In the present study, the list of potential targets of triptolide was analyzed with a functional annotation protocol provided by DAVID Bioinformatics Resources (version 6.7). The whole Brookhaven PDB database was used as a background data set during the enrichment analysis to avoid bias caused by well-studied proteins.

Molecular docking of triptolide in complex with holo-ATP-p38α. Crystal coordinates of active p38α in complex with ATP were obtained from data reported under PDB accession number 2GFS (53). We used the Surflex-Dock program, a program widely used to calculate protein-ligand interactions as well as to efficiently predict active conformations (54). The Protomol-based method, an object-oriented molecular dynamics simulation approach, and an empirical scoring function in Surflex-Dock were used to dock triptolide into the binding site of holo-ATP-p38α. The Protomol was generated by using a non-ligand-based approach. During the Protomol generation process, two parameters, Protomol_bloat and the Protomol_threshold, are critical for the formation of an appropriate binding pocket. Protomol_bloat determines how far the site should extend from a potential ligand, and Protomol_threshold determines how deep the atomic probes that are used to define the Protomol can penetrate into the protein. Default values of a Protomol_bloat value of 0 and a Protomol_threshold value of 0.5 were sufficient to obtain reasonable binding pockets for triptolide docking to holo-ATP-p38α. The default values of all the other parameters were also assigned. The docking score was calculated by using the Surflex-Dock scoring function, considering the factors important in the ligand-receptor interaction, including the hydrophobic, polar, repulsive, entropic, and solvation terms. The highest-scoring conformation of a potent compound, based on the Surflex-Dock scoring functions, was selected as the final bioactive conformation.

Phosphor Explorer antibody array analysis. For the protein antibody array analysis, H460 cells were treated with triptolide (50 nM for 16 h). Total proteins were extracted from cells in a pool from three independent experiments for the treated and control groups using an antibody array assay kit (Full Moon Biosystems, Sunnyvale, CA). The Phosphor Explorer antibody array (Full Moon Biosystems) was used to define the protein phosphorylation profile, according to the supplier's instructions. The array was scanned by using the Agilent microarray scanner (Agilent Technologies, Santa Clara, CA), and the data were extracted and analyzed by using Agilent Feature Extraction software (Agilent Technologies). The downstream protein substrates of a protein kinase were based on data from a database provided by the PhosphoNetworks website (http://www.phosphonetworks.org/) and other sources (55, 56).

Histopathology. We fixed tissues in 10% formalin and stained the tissue sections with hematoxylin and eosin (H&E) or by immunohistochemistry (IHC). For IHC, paraffin-embedded 5-μm tissue sections were deparaffinized, rehydrated, and stained with specific antibodies against NF-κB (Santa Cruz Biotechnology Inc.) and CD68 (Abcam). All H&E and IHC assays were performed by the City of Hope Pathology Core according to standard protocols.

Accession number(s). The microarray data have been deposited in the GEO database under accession number GSE99514.

ACKNOWLEDGMENTS

We thank the Integrative Functional Genomics, Light Microscopy, and Pathology Core Facilities at City of Hope for their assistance with the microarray gene expression,

histopathology, and immunofluorescence analyses. We thank Nancy Linford for editorial assistance.

The core facilities at City of Hope were partly supported by a Cancer Center Support Grant (CCSG) awarded by the National Cancer Institute under award number P30CA033572. This work was supported by NIH grants R01CA085344 to B.S., R50CA211397 to L.Z., and 5K12CA001727-20 to D.J.R.

We declare no conflicts of interest in this study.

L.Z. designed and conducted biochemical and mouse phenotype analyses and contributed to manuscript preparation. H.D., L.W., J.L., M.Q., M.Z., L.H., J.L., X.C., and L.C. conducted biochemical and cellular assays and conducted anatomic analyses of mice. J.J. conducted molecular modeling to identify potential targets of triptolide. J.Y.K. and K.R. coordinated and supervised the pathological and histological analyses and contributed to manuscript preparation. Z.X. and D.J.R. designed and supervised experiments in this study and contributed to manuscript preparation. B.S. supervised the entire project, designed and coordinated most of the experiments in this study, and contributed to manuscript preparation.

REFERENCES

1. Hanahan D, Weinberg RA. 2011. Hallmarks of cancer: the next generation. Cell 144:646–674. https://doi.org/10.1016/j.cell.2011.02.013.
2. Coussens LM, Werb Z. 2002. Inflammation and cancer. Nature 420:860–867. https://doi.org/10.1038/nature01322.
3. Grivennikov SI, Greten FR, Karin M. 2010. Immunity, inflammation, and cancer. Cell 140:883–899. https://doi.org/10.1016/j.cell.2010.01.025.
4. Dinarello CA. 2000. Proinflammatory cytokines. Chest 118:503–508. https://doi.org/10.1378/chest.118.2.503.
5. Chiu YH, Zhao M, Chen ZJ. 2009. Ubiquitin in NF-kappaB signaling. Chem Rev 109:1549–1560. https://doi.org/10.1021/cr800554j.
6. Ghosh S, Karin M. 2002. Missing pieces in the NF-kappaB puzzle. Cell 109(Suppl):S81–S96. https://doi.org/10.1016/S0092-8674(02)00703-1.
7. Greten FR, Eckmann L, Greten TF, Park JM, Li ZW, Egan LJ, Kagnoff MF, Karin M. 2004. IKKbeta links inflammation and tumorigenesis in a mouse model of colitis-associated cancer. Cell 118:285–296. https://doi.org/10.1016/j.cell.2004.07.013.
8. Pikarsky E, Porat RM, Stein I, Abramovitch R, Amit S, Kasem S, Gutkovich-Pyest E, Urieli-Shoval S, Galun E, Ben-Neriah Y. 2004. NF-kappaB functions as a tumour promoter in inflammation-associated cancer. Nature 431:461–466. https://doi.org/10.1038/nature02924.
9. Zheng L, Dai H, Zhou M, Li M, Singh P, Qiu J, Tsark W, Huang Q, Kernstine K, Zhang X, Lin D, Shen B. 2007. Fen1 mutations result in autoimmunity, chronic inflammation and cancers. Nat Med 13:812–819. https://doi.org/10.1038/nm1599.
10. Coussens LM, Zitvogel L, Palucka AK. 2013. Neutralizing tumor-promoting chronic inflammation: a magic bullet? Science 339:286–291. https://doi.org/10.1126/science.1232227.
11. Su D, Song Y, Li R. 1990. Comparative clinical study of rheumatoid arthritis treated by triptolide and an ethyl acetate extract of Tripterygium wilfordii. Zhong Xi Yi Jie He Za Zhi 10:144–146. (In Chinese.)
12. Lee KY, Park JS, Jee YK, Rosen GD. 2002. Triptolide sensitizes lung cancer cells to TNF-related apoptosis-inducing ligand (TRAIL)-induced apoptosis by inhibition of NF-kappaB activation. Exp Mol Med 34:462–468. https://doi.org/10.1038/emm.2002.64.
13. Phillips PA, Dudeja V, McCarroll JA, Borja-Cacho D, Dawra RK, Grizzle WE, Vickers SM, Saluja AK. 2007. Triptolide induces pancreatic cancer cell death via inhibition of heat shock protein 70. Cancer Res 67:9407–9416. https://doi.org/10.1158/0008-5472.CAN-07-1077.
14. Manzo SG, Zhou ZL, Wang YQ, Marinello J, He JX, Li YC, Ding J, Capranico G, Miao ZH. 2012. Natural product triptolide mediates cancer cell death by triggering CDK7-dependent degradation of RNA polymerase II. Cancer Res 72:5363–5373. https://doi.org/10.1158/0008-5472.CAN-12-1006.
15. Chugh R, Sangwan V, Patil SP, Dudeja V, Dawra RK, Banerjee S, Schumacher RJ, Blazar BR, Georg GI, Vickers SM, Saluja AK. 2012. A preclinical evaluation of minnelide as a therapeutic agent against pancreatic cancer. Sci Transl Med 4:156ra139. https://doi.org/10.1126/scitranslmed.3004334.
16. Deng L, Wang C, Spencer E, Yang L, Braun A, You J, Slaughter C, Pickart C, Chen ZJ. 2000. Activation of the IkappaB kinase complex by TRAF6 requires a dimeric ubiquitin-conjugating enzyme complex and a unique polyubiquitin chain. Cell 103:351–361. https://doi.org/10.1016/S0092-8674(00)00126-4.
17. Kopp E, Ghosh S. 1994. Inhibition of NF-kappa B by sodium salicylate and aspirin. Science 265:956–959. https://doi.org/10.1126/science.8052854.
18. Xia Y, Padre RC, De Mendoza TH, Bottero V, Tergaonkar VB, Verma IM. 2009. Phosphorylation of p53 by IkappaB kinase 2 promotes its degradation by beta-TrCP. Proc Natl Acad Sci U S A 106:2629–2634. https://doi.org/10.1073/pnas.0812256106.
19. Titov DV, Gilman B, He QL, Bhat S, Low WK, Dang Y, Smeaton M, Demain AL, Miller PS, Kugel JF, Goodrich JA, Liu JO. 2011. XPB, a subunit of TFIIH, is a target of the natural product triptolide. Nat Chem Biol 7:182–188. https://doi.org/10.1038/nchembio.522.
20. Tibbetts RS, Brumbaugh KM, Williams JM, Sarkaria JN, Cliby WA, Shieh SY, Taya Y, Prives C, Abraham RT. 1999. A role for ATR in the DNA damage-induced phosphorylation of p53. Genes Dev 13:152–157. https://doi.org/10.1101/gad.13.2.152.
21. Shieh SY, Ikeda M, Taya Y, Prives C. 1997. DNA damage-induced phosphorylation of p53 alleviates inhibition by MDM2. Cell 91:325–334. https://doi.org/10.1016/S0092-8674(00)80416-X.
22. Ashcroft M, Kubbutat MH, Vousden KH. 1999. Regulation of p53 function and stability by phosphorylation. Mol Cell Biol 19:1751–1758. https://doi.org/10.1128/MCB.19.3.1751.
23. She QB, Chen N, Dong Z. 2000. ERKs and p38 kinase phosphorylate p53 protein at serine 15 in response to UV radiation. J Biol Chem 275:20444–20449. https://doi.org/10.1074/jbc.M001020200.
24. Sun P, Yoshizuka N, New L, Moser BA, Li Y, Liao R, Xie C, Chen J, Deng Q, Yamout M, Dong MQ, Frangou CG, Yates JR, III, Wright PE, Han J. 2007. PRAK is essential for ras-induced senescence and tumor suppression. Cell 128:295–308. https://doi.org/10.1016/j.cell.2006.11.050.
25. Cuenda A, Rouse J, Doza YN, Meier R, Cohen P, Gallagher TF, Young PR, Lee JC. 1995. SB 203580 is a specific inhibitor of a MAP kinase homologue which is stimulated by cellular stresses and interleukin-1. FEBS Lett 364:229–233. https://doi.org/10.1016/0014-5793(95)00357-F.
26. Duncia JV, Santella JB, III, Higley CA, Pitts WJ, Wityak J, Frietze WE, Rankin FW, Sun JH, Earl RA, Tabaka AC, Teleha CA, Blom KF, Favata MF, Manos EJ, Daulerio AJ, Stradley DA, Horiuchi K, Copeland RA, Scherle PA, Trzaskos JM, Magolda RL, Trainor GL, Wexler RR, Hobbs FW, Olson RE. 1998. MEK inhibitors: the chemistry and biological activity of U0126, its analogs, and cyclization products. Bioorg Med Chem Lett 8:2839–2844. https://doi.org/10.1016/S0960-894X(98)00522-8.
27. Siegel R, Ma J, Zou Z, Jemal A. 2014. Cancer statistics, 2014. CA Cancer J Clin 64:9–29. https://doi.org/10.3322/caac.21208.
28. Haegens A, van der Vliet A, Butnor KJ, Heintz N, Taatjes D, Hemenway D, Vacek P, Freeman BA, Hazen SL, Brennan ML, Mossman BT. 2005. Asbestos-induced lung inflammation and epithelial cell proliferation are altered in myeloperoxidase-null mice. Cancer Res 65:9670–9677. https://doi.org/10.1158/0008-5472.CAN-05-1751.
29. Malkinson AM. 2005. Role of inflammation in mouse lung

tumorigenesis: a review. Exp Lung Res 31:57–82. https://doi.org/10.1080/01902140490495020.
30. Harris RE, Beebe-Donk J, Schuller HM. 2002. Chemoprevention of lung cancer by non-steroidal anti-inflammatory drugs among cigarette smokers. Oncol Rep 9:693–695.
31. Lee JM, Yanagawa J, Peebles KA, Sharma S, Mao JT, Dubinett SM. 2008. Inflammation in lung carcinogenesis: new targets for lung cancer chemoprevention and treatment. Crit Rev Oncol Hematol 66:208–217. https://doi.org/10.1016/j.critrevonc.2008.01.004.
32. Holmes MD, Chen WY, Li L, Hertzmark E, Spiegelman D, Hankinson SE. 2010. Aspirin intake and survival after breast cancer. J Clin Oncol 28:1467–1472. https://doi.org/10.1200/JCO.2009.22.7918.
33. Al Hadidi S. 2016. Aspirin and cancer risk. JAMA Oncol 2:1371–1372. https://doi.org/10.1001/jamaoncol.2016.2332.
34. Cao Y, Nishihara R, Wu K, Wang M, Ogino S, Willett WC, Spiegelman D, Fuchs CS, Giovannucci EL, Chan AT. 2016. Population-wide impact of long-term use of aspirin and the risk for cancer. JAMA Oncol 2:762–769. https://doi.org/10.1001/jamaoncol.2015.6396.
35. Bartkova J, Horejsi Z, Koed K, Kramer A, Tort F, Zieger K, Guldberg P, Sehested M, Nesland JM, Lukas C, Orntoft T, Lukas J, Bartek J. 2005. DNA damage response as a candidate anti-cancer barrier in early human tumorigenesis. Nature 434:864–870. https://doi.org/10.1038/nature03482.
36. Zheng L, Dai H, Zhou M, Li X, Liu C, Guo Z, Wu X, Wu J, Wang C, Zhong J, Huang Q, Garcia-Aguilar J, Pfeifer GP, Shen B. 2012. Polyploid cells rewire DNA damage response networks to overcome replication stress-induced barriers for tumour progression. Nat Commun 3:815. https://doi.org/10.1038/ncomms1825.
37. Rath PC, Aggarwal BB. 1999. TNF-induced signaling in apoptosis. J Clin Immunol 19:350–364. https://doi.org/10.1023/A:1020546615229.
38. Karin M, Cao Y, Greten FR, Li ZW. 2002. NF-kappaB in cancer: from innocent bystander to major culprit. Nat Rev Cancer 2:301–310. https://doi.org/10.1038/nrc780.
39. Liu H, Liu ZH, Chen ZH, Yang JW, Li LS. 2000. Triptolide: a potent inhibitor of NF-kappa B in T-lymphocytes. Acta Pharmacol Sin 21:782–786.
40. Jiang XH, Wong BC, Lin MC, Zhu GH, Kung HF, Jiang SH, Yang D, Lam SK. 2001. Functional p53 is required for triptolide-induced apoptosis and AP-1 and nuclear factor-kappaB activation in gastric cancer cells. Oncogene 20:8009–8018. https://doi.org/10.1038/sj.onc.1204981.
41. Lin N, Sato T, Ito A. 2001. Triptolide, a novel diterpenoid triepoxide from Tripterygium wilfordii Hook. f., suppresses the production and gene expression of pro-matrix metalloproteinases 1 and 3 and augments those of tissue inhibitors of metalloproteinases 1 and 2 in human synovial fibroblasts. Arthritis Rheum 44:2193–2200. https://doi.org/10.1002/1529-0131(200109)44:9<2193::AID-ART373>3.0.CO;2-5.
42. Webster GA, Perkins ND. 1999. Transcriptional cross talk between NF-kappaB and p53. Mol Cell Biol 19:3485–3495. https://doi.org/10.1128/MCB.19.5.3485.
43. Cooks T, Pateras IS, Tarcic O, Solomon H, Schetter AJ, Wilder S, Lozano G, Pikarsky E, Forshew T, Rosenfeld N, Harpaz N, Itzkowitz S, Harris CC, Rotter V, Gorgoulis VG, Oren M. 2013. Mutant p53 prolongs NF-kappaB activation and promotes chronic inflammation and inflammation-associated colorectal cancer. Cancer Cell 23:634–646. https://doi.org/10.1016/j.ccr.2013.03.022.
44. Hawkey CJ. 1999. COX-2 inhibitors. Lancet 353:307–314. https://doi.org/10.1016/S0140-6736(98)12154-2.
45. Dar AC, Shokat KM. 2011. The evolution of protein kinase inhibitors from antagonists to agonists of cellular signaling. Annu Rev Biochem 80:769–795. https://doi.org/10.1146/annurev-biochem-090308-173656.
46. Lu Y, Zhang Y, Li L, Feng X, Ding S, Zheng W, Li J, Shen P. 2014. TAB1: a target of triptolide in macrophages. Chem Biol 21:246–256. https://doi.org/10.1016/j.chembiol.2013.12.009.
47. Park B, Sung B, Yadav VR, Chaturvedi MM, Aggarwal BB. 2011. Triptolide, histone acetyltransferase inhibitor, suppresses growth and chemosensitizes leukemic cells through inhibition of gene expression regulated by TNF-TNFR1-TRADD-TRAF2-NIK-TAK1-IKK pathway. Biochem Pharmacol 82:1134–1144. https://doi.org/10.1016/j.bcp.2011.07.062.
48. Tomayko MM, Reynolds CP. 1989. Determination of subcutaneous tumor size in athymic (nude) mice. Cancer Chemother Pharmacol 24:148–154. https://doi.org/10.1007/BF00300234.
49. Chung L, Onyango D, Guo Z, Jia P, Dai H, Liu S, Zhou M, Lin W, Pang I, Li H, Yuan YC, Huang Q, Zheng L, Lopes J, Nicolas A, Chai W, Raz D, Reckamp KL, Shen B. 2014. The FEN1 E359K germline mutation disrupts the FEN1-WRN interaction and FEN1 GEN activity, causing aneuploidy-associated cancers. Oncogene 34:902–911. https://doi.org/10.1038/onc.2014.19.
50. Zheng L, Dai H, Qiu J, Huang Q, Shen B. 2007. Disruption of the FEN-1/PCNA interaction results in DNA replication defects, pulmonary hypoplasia, pancytopenia, and newborn lethality in mice. Mol Cell Biol 27:3176–3186. https://doi.org/10.1128/MCB.01652-06.
51. Ran FA, Hsu PD, Wright J, Agarwala V, Scott DA, Zhang F. 2013. Genome engineering using the CRISPR-Cas9 system. Nat Protoc 8:2281–2308. https://doi.org/10.1038/nprot.2013.143.
52. Chen YZ, Zhi DG. 2001. Ligand-protein inverse docking and its potential use in the computer search of protein targets of a small molecule. Proteins 43:217–226. https://doi.org/10.1002/1097-0134(20010501)43:2<217::AID-PROT1032>3.0.CO;2-G.
53. Goldstein DM, Alfredson T, Bertrand J, Browner MF, Clifford K, Dalrymple SA, Dunn J, Freire-Moar J, Harris S, Labadie SS, La Fargue J, Lapierre JM, Larrabee S, Li F, Papp E, McWeeney D, Ramesha C, Roberts R, Rotstein D, San Pablo B, Sjogren EB, So OY, Talamas FX, Tao W, Trejo A, Villasenor A, Welch M, Welch T, Weller P, Whiteley PE, Young K, Zipfel S. 2006. Discovery of S-[5-amino-1-(4-fluorophenyl)-1H-pyrazol-4-yl]-[3-(2,3-dihydroxypropoxy)phenyl]me thanone (RO3201195), an orally bioavailable and highly selective inhibitor of p38 MAP kinase. J Med Chem 49:1562–1575. https://doi.org/10.1021/jm050736c.
54. Jain AN. 2003. Surflex: fully automatic flexible molecular docking using a molecular similarity-based search engine. J Med Chem 46:499–511. https://doi.org/10.1021/jm020406h.
55. Lu Z, Xu S. 2006. ERK1/2 MAP kinases in cell survival and apoptosis. IUBMB Life 58:621–631. https://doi.org/10.1080/15216540600957438.
56. Trempolec N, Dave-Coll N, Nebreda AR. 2013. SnapShot: p38 MAPK substrates. Cell 152:924. https://doi.org/10.1016/j.cell.2013.01.047.